This paper describes the main advantages of hydrostatic dynamic bearings of the double type, which have several lubricant films. It is indicated that they have an increased carrying capacity, by 1.8 times, and an extended range of stable operation, by 1.5 times, compared to conventional sleeve bearings with one lubricating film. The importance of determining the thickness of the bearing disk has been demonstrated, as it affects its durability. The goal was to investigate the impact of changes in the operational and structural parameters of a double bearing on the thickness of its disk. A sequence for determining the disk thickness has been proposed, including a joint solution to Reynolds equations, the balance of work fluid flow rate, as well as determining the loads acting on a bearing disk, which makes it possible to rationally assign the thickness of the bearing disk. The most common and effective methods of successive approximations have been used in the numerical implementation of Reynolds equations and flow rate balances. The action of centrifugal forces caused by the rotation of the disk has been taken into consideration in determining the total load acting on the bearing disk. The bending strength of the bearing disk was considered under its exposure to the total load. It was noted that due to the high flow rate of the working liquid pumped through the bearing, and the small change in the temperature of the liquid inside the bearing, the temperature deformations of the disk were not taken into consideration. The magnitude of change in the thickness of the double bearing disk has been determined, caused by the action of centrifugal forces in the examined range of angular speeds of the disk's rotation with the shaft.

The reported results could be especially useful in the design of rotor supports for nuclear power plants where bearings have large dimensions, as well as for other units in power plants

Keywords: hydrostatic dynamic bearing, disk thickness, eccentricity, centrifugal forces, bending stiffness

UDC 621.822.5.032:532.517.4
DOI: 10.15587/1729-4061.2021.235284

DETERMINING THE INFLUENCE OF STRUCTURAL AND OPERATIONAL PARAMETERS OF A DOUBLE BEARING ON THE THICKNESS OF ITS DISC

Vladimir Nazin
Doctor of Technical Sciences
Department of Theoretical Mechanics, Mechanical Engineering and Robotic Mechanical Systems
National Aerospace University "Kharkiv Aviation Institute"
Chkalova str., 17, Kharkiv, Ukraine, 61070
E-mail: v.nazin@khai.edu

Received date 22.04.2021
Accepted date 26.05.2021
Published date 30.06.2021

How to Cite: *Nazin, V. (2021). Determining the influence of structural and operational parameters of a double bearing on the thickness of its disc. Eastern-European Journal of Enterprise Technologies, 3 (7 (111)), 68–73. doi: https://doi.org/10.15587/1729-4061.2021.235284*

1. Introduction

The durability of machines depends on many factors, including the reliable operation of the supports of their rotors. Experience shows that the weakest nodes of turbomachines are supports. For example, among turbine damage that requires an immediate shutdown, the damage to bearings accounts for 17.7 %. In centrifugal compressors, about 16 % of all faults are failures of support bearings.

Both rolling bearings and sliding bearings are widely used in rotor supports. Due to the increasing rotation speeds of the rotors in modern machines, the application of sliding bearings is constantly expanding. In some cases, the use of rolling bearings is simply impossible, for example, in the supports of cranked shafts. Among the sliding bearings, liquid friction sliding bearings occupy an important place. The machines and units of power plants always use different types of liquid materials, which are convenient to use as working bodies for rotor support. In this case, the most appropriate is to apply hydrostatic dynamic bearings, which could work on any liquid lubricants, including the working bodies of machines. These bearings are almost non-wearable, except for the initial moments of the launch and the end of stopping. The use of hydrostatic dynamic bearings expands the range of materials used. The diametric dimensions of hydrostatic dynamic bearings are also smaller than those of the rolling bearings. Unlike rolling bearings, which have discrete standard diameters, hydrostatic dynamic sliding bearings could be made with any diameter.

Liquid friction sliding bearings, designed for the rotors of nuclear power plant turbines, could work on the working bodies of turbines. The loads that act on bearings in these power plants are tens of tons; the bearings have diameter sizes of 800 mm or more, the circular speeds in these bearings reach 100 m/s. High sliding speeds and the existence of residual imbalance of machines' rotors lead to an increase in the vibration overloads and in the amplitude of rotor oscillations.

The design of double hydrostatic dynamic bearings is very promising for the modern working conditions of machines and power plant assemblies [1]. Unlike conventional sleeve bearings, they have several lubricants (bearing) films and, therefore, possess an increased carrying capacity, by about 1.8 times [2], and an extended range of stable operation, by about 1.41 times [3].

Given the novelty and lack of detailed studies, and considering the prospects of the proposed hydrostatic dynamic bearings of the double type, it is a relevant task to analyze their performance.

2. Literature review and problem statement

Work [4] examines the sliding bearings operated under a hydrodynamic friction mode. On ships and submarines, pro-

pellers are often equipped with water grease bearings. The authors report the results of an experimental study into the effect of rotational speed on work eccentricity, the friction factor, and lubricant modes.

The reliability of such a bearing would be less in comparison with the hydrostatic dynamic bearing, which employs both the hydrodynamic and hydrostatic effects. Work [5] gives a computational model for analyzing the operation of self-installed support bearings with a sloping pillow. By self-installing the pillows, the reliability of the bearing is improved. However, the presence of contact pressures and the resulting Hertz stresses reduces the reliability of the bearing. Paper [6] notes that the total cost of friction and wear is EUR 250 billion a year worldwide. The results from testing the sliding bearings operated using a special mesogenic fluid are presented. This liquid reduces the friction factor by 60 %. However, the application of these liquids reduces friction but does not eliminate it. Work [7] shows the effectiveness of micro texturing on tribological characteristics. That has reduced the friction factor and increased contact load in under-lubricated conditions. Insufficient lubrication also reduces the operational reliability of the bearing. Paper [8] reports a study into the sliding bearing in a hydraulic pump powered by seawater. The bearing operates under the conditions of semi-dry and boundary friction, which reduces its durability. Work [9] describes a study into the effect of basic parameters on resistance to the friction of sliding bearings. It is shown that the main influence on friction is exerted by the speed of rotation of the pin, the sliding factor of the oil film, and the pressure at the input and output of the bearing. Noteworthy is work [10], which offers hybrid bearings that are a combination of rolling bearings and film bearings to improve operational performance. The cited work reports the results from the theoretical and numerical studies. The conditions for minimal friction effect were justified. Paper [11] gives the characteristics of the slip at the combined effect of fluid inertia and fluid slippage at the interface boundary between the fluid and solid body. The studies have shown that the effect of fluid slippage is more important than fluid inertia. Paper [12] describes a program to analyze the hydrodynamics of cylindrical sliding bearings. A two-dimensional problem of the lubricating flow is considered, accounting for the different types of deviations of the contact surface from the cylindrical shape. The work surface is divided into several zones of hydrodynamic friction. Work [13] examines the frictional properties of a wide range of base liquids at three temperatures and two pressures. The studies show that the molecular structure of working fluid plays an important role in friction loss. The work that is closest to the problem discussed in this paper is [14], in which the design of a hydrostatic dynamic bearing of the double type is considered. The cited work recommends the thickness of the disk in a double-type bearing. However, the recommendation is not supported by calculations of disk thickness. That necessitated devising a procedure for calculating the thickness of the disk in a double-type bearing. The quantitative assessment of the disk thickness under different operational conditions makes it possible to significantly improve the static and dynamic characteristics of the bearing, as well as improve its reliability and durability.

3. The aim and objectives of the study

The aim of this work is to identify the impact of change in the operational and structural parameters of the bearing on the thickness of its disk, which would optimize the thickness of the disk and influence the carrying capacity and the limit of the bearing stable operation.

To accomplish the aim, the following tasks have been set:

– to construct and solve an equation to calculate the thickness of the disk, which takes into consideration the effect of hydrodynamic and centrifugal forces;

– to determine the magnitude of the impact of the ratio of hydrodynamic and centrifugal forces on the thickness of the disk at different operational and geometric parameters of the dual bearing.

4. The study materials and methods

When deriving theoretical dependences, the laws of hydromechanics and hydraulics were used to determine the thickness of the dual hydrostatic dynamic bearing disk. The flow rate of working fluid through the input compensating devices was recorded using the hydraulic formula. The flow rate along the contour of the carrying chambers was recorded taking into consideration the portable and gradient friction of the working fluid. The Reynolds equation was used to determine the function of pressure change at inter-chamber partitions, which was recorded taking into consideration assumptions common in hydrodynamic theory. The Navier-Stokes equations and the solidity equation were used to write down the specialized form of the Reynolds equation. When the Reynolds equation was generalized for the case of a developed turbulent flow of the working fluid, time-resolved values of velocities and pressures were used instead of instantaneous. The V.N. Constantinescu method was chosen among known techniques of accounting for the turbulence of a working fluid flow. In the numerical implementation of the devised procedure for calculating the thickness of the dual bearing disk, a method of final differences was used in combination with the longitudinal-transverse sweep method. The numerical implementation of the devised disk thickness calculation procedure was carried out using MS Excel software. The drawings and charts showing the results were built in the Compass graphic editor.

5. The results of studying the disk thickness

5. 1. Constructing and solving an equation to calculate the disk thickness, which takes into consideration the effect of hydrodynamic and centrifugal forces

The hydrostatic dynamic double-type bearing under consideration includes disk 1 (Fig. 1), mounted motionless onto shaft 2, and rotating with it.

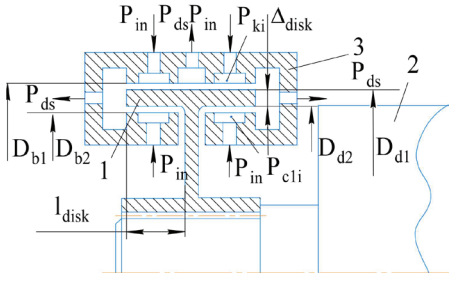

Fig. 1. Schematic showing the radial hydrostatic dynamic bearing: 1 – bearing; 2 – disk; 3 – shaft

The outer rim of the disk is extended, which makes it possible to feed a working liquid from both the outer and inside of the disk and, thus, form dual hydrostatic dynamic bearing 3 with several layers of lubricant. There is a necessary gap between the work surfaces of the disk and bearing. At the work surfaces of the bearing (outer and inner), carrying chambers are installed (the pressure in them is indicated by P_{ci} and P_{c1i}), to which, under pressure P_{in}, a working liquid is fed. At the input to the chambers, input pressure compensators are installed of the jet type. After passing through the slit tract of the bearing, a working liquid is discharged at pressure P_{ds} (Fig. 1). Under the external load, the center of the disk shifts relative to the center of the bearing to a certain size, which is termed the bearing eccentricity. At the same time, in the outer part of the bearing, in the lower chambers, the pressure increases as the gap has decreased here, and, in the upper chambers, the pressure decreases due to the increase in the gap. This creates a carrying capacity in the outer part of the bearing. In the inner parts of the bearing, on the contrary, in the upper chambers – the pressure increases as the gap has increased there, and, in the lower chambers, the pressure decreases due to the increase in the gap. This creates a carrying capacity in the inner parts of the bearing. The carrying capacities of the outer and inner parts of the bearing are summed up as they are directed to one side. Therefore, the bearing capacity of the double bearing is much greater than the carrying capacity of a single sleeve bearing with one lubricating layer. In the case of a constant load, the main characteristics of the bearing are the carrying capacity, the flow rate of a working liquid, and the loss of power for friction and pumping. Underlying these characteristics is the pressure distribution function related to a working fluid layer.

Calculating the thickness of a dual hydrostatic dynamic bearing disk involves determining the forces acting on it.

The theory of hydrostatic dynamic bearing of the double type is considered in a stationary statement. Determining the hydrodynamic forces acting on the disk relates to a joint solution to the Reynolds equations and flow rate balance equations.

Details in determining the hydrodynamic forces in the dual bearing are given in work [15].

The flow rate balance equations are written for the outer and inner parts of the bearing based on the conditions of the equality of flow rates through the input compensating devices, the type of jets, and the flow rate along the contour of the i-th chamber (Fig. 2).

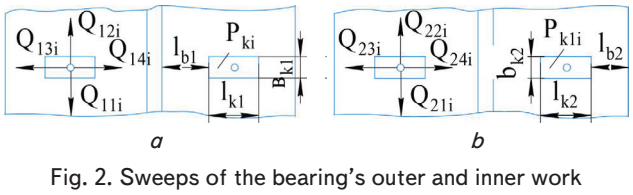

Fig. 2. Sweeps of the bearing's outer and inner work surfaces: *a* – the outer surface of the bearing; *b* – the inner surface of the bearing

In Fig. 2, the following working fluid flow rates are indicated:

– Q_{11i}, Q_{12i}, Q_{13i}, Q_{14i} – the flow rate along the i-th chamber contour for the outer part of the bearing surface;

– Q_{21i}, Q_{22i}, Q_{23i}, Q_{24i} – the flow rate along the i-th chamber contour for the inside of the bearing's work surface.

The pressure in the chambers of the outer and inner parts of the bearing is indicated by P_{Ki} and P_{K1i}. As regards the area of the chamber, these pressures were adopted constant. Fig. 2 also shows the size of the chambers and the distance from them to the ends of the bearing.

The flow rate along the i-th chamber contour was recorded taking into consideration the portable and gradient currents of the working fluid. The expressions for flow rates were generalized for the case of a developed turbulent flow of the working fluid using turbulence ratios. Turbulence ratios were determined using the most common method [16–18].

The flow rate balance equations were solved by an iterative method until the required solution accuracy was achieved.

To determine the function of a pressure change at the inter-chamber partitions, the Reynolds equation was solved, which was recorded taking into consideration the following assumptions common in hydrodynamic theory:

1. The grease flow is isothermal.
2. Grease is an incompressible Newtonian liquid.
3. The inaccuracies of the manufacture and assembly of bearing parts, as well as their deformations caused by grease pressure and heating, are negligible.
4. There is no cavitation in the working fluid, and there is no fluid-solid sliding at the boundary of the section.
5. Pressure gradients by film thickness are small compared to the pressure gradient in other directions.
6. The effect of mass forces is not essential.
7. The pressure in the chambers is the same on their surface.
8. The thickness of the lubricant layer is small compared to the radii and the length of the bearing, so the curvature of the bearing surface could be neglected; one can apply the cartesian coordinates instead of curvilinear.
9. The inertial terms of the Navier-Stokes equations are small compared to the viscous.

Reynolds' equations do not have an exact analytical solution. Therefore, an approximate numerical method was used to solve them.

One of these techniques is the method of finite differences in combination with the longitudinal-transverse sweep method [19]. The numerical implementation employed difference schemes recorded in an implicit form. Compared to explicit, they are more stable and do not require a rigid restriction on the step of the grid. At the same time, the systems of algebraic equations were solved.

A solution to the problem in the sweep method is derived in the following form:

$$\bar{P}_i = \alpha_i \cdot \bar{P}_{i+1} + \beta_i, \tag{1}$$

where i=2, 3, ..., N–1 is the grid node numbers; α_i, β_i are the sweep coefficients determined from the following formulas:

$$\alpha_i = -\frac{A_i}{B_i + C_i \cdot \alpha_{i-1}}; \quad \beta_i = \frac{F_i - C_i \cdot \beta_{i-1}}{B_i + C_i \cdot \alpha_{i-1}}. \tag{2}$$

The basic idea of the longitudinal-transverse sweep method is to reduce the transition from layer to layer to solving sequentially the one-dimensional problems along the rows and along the columns. In addition to the main values of the grid function $\bar{P}_n$ and $\bar{P}_{n+1}$, an intermediate value $\bar{P}_{n+1/2}$ is introduced on the sublayer. The transition from the n-th layer to the n+1-th layer takes place in two stages.

By setting the initial pressure values in the grid nodes, the pressure values in the grid nodes are determined at the

next step by the longitudinal-transverse sweep method. The iterative process continues until the specified accuracy is obtained

$$\left|\left(\bar{P}_{i,j}\right)_{n+1}-\left(\bar{P}_{i,j}\right)_{n}\right|\le\varepsilon_2,$$

where ε_2 is the accuracy in determining the pressure at the inter-chamber partition.

The known pressures in the chambers and inter-chamber partition nodes were used to determine the bearing's carrying capacity.

The carrying capacity was determined as the sum of the carrying capacities of the outer and inner working surfaces; and the carrying capacities of the outer and inner surfaces of the bearing were determined as the sum of the carrying capacities of the chambers, as well as the inter-chamber and end partitions.

In addition to hydrodynamic forces, the disk is exposed to the forces of inertia induced by its rotation F_{cen}.

$$F_{cen}=m\cdot\omega^2\cdot r. \quad (3)$$

where ω is the disk rotation angular velocity;

$r=\frac{D_{D1}+D_{D2}}{4}$ is the disk rim mean diameter;

D_{D1} is the disk outer diameter (Fig. 1);

D_{D2} is the disk inner diameter;

$m=\frac{V\cdot\gamma_{sp}}{g}$ is the disk rim mass;

$V=\frac{\pi}{4}\left(D_{D1}^2-D_{D2}^2\right)\cdot\ell_{disk}$ is the disk console part volume;

γ_{sp} is the disk material's specific weight;

g=9.86 m/s^2 is the free-fall acceleration;

ℓ_{disk} is the disk console part length (Fig. 1).

The minimum thickness of the disk was determined based on the condition of its strength at bending under the influence of hydrodynamic forces and the forces of inertia of the disk induced by its rotation:

$$\Delta_{disk}=\frac{\left(i_\Sigma+F_{cen}\right)\cdot l_{disk}}{\pi\cdot R_{D1}^2\cdot 0,25\cdot\sigma_d}, \quad (4)$$

where σ_B is the limit of the strength of the disk material.

The small-diameter bearing under consideration had the following geometric and working parameters (Fig. 1):

1. Feed pressure P_{in}=1 MPa.
2. The angular velocity of the disk with a shaft ω=314 s^{-1}.
3. Bearing's outer diameter D_{b1}=0.091 m.
4. Bearing's inner diameter D_{b2}=0.083 m.
5. Disk outer diameter D_{D1}=0.09082 m.
6. Disk inner diameter D_{D2}=0.08318 m.
7. Jet device diameter d_{jet1}=d_{jet2}=0.0012 m.
8. Working fluid is the water at 20 °C.
9. The eccentricity of the shaft with a disk in the bearing e_0=0.00007 m.
10. Disk console length ℓ_{disk}=0.025 m.

The results of calculating the disk thickness Δ_{disk} for various materials used in its manufacture are shown in Fig. 3.

The calculation shows that with an increase in feed pressure from 1 MPa to 8 MPa, the disk thickness increases by about 6 times; and the influence of the disk material on its thickness revealed that the thickness of the disk increases with a decrease in the strength of the material from which the disk is made.

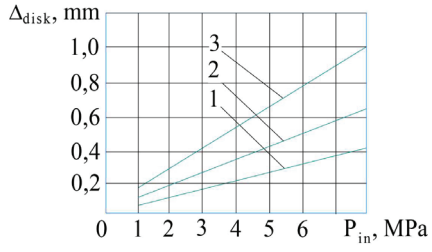

Fig. 3. The effect of feed pressure P_{in} on disk thickness Δ_{disk} for various disk's materials disregarding the centrifugal forces: 1 – steel; 2 – bronze; 3 – aluminum

At a feed pressure of 1 MPa, the steel disk's thickness is 2.5 times less than the thickness of the aluminum disk. As the feed pressure increases, the ratio of aluminum and steel thicknesses decreases. At a feed pressure of 8 MPa, the steel disk is 2.5 times thicker compared to the thickness of an aluminum disk.

The linear nature of the dependence of the thickness of the disk on the feed pressure is explained by the fact that under the assumptions common in the hydrodynamic lubricant theory, the dependence of the bearing's carrying capacity on feed pressure would be linear. This fact is confirmed by the experimental studies conducted for hydrostatic dynamic bearings.

A bearing of the larger diameter had the following parameters:

1. Bearing's outer diameter D_{d1}=0.45 m.
2. Bearing's outer diameter D_{d2}=0.43956 m.
3. Disk outer diameter D_{D1}=0.44978 m.
4. Disk outer diameter D_{D2}=0.43978 m.
5. Gaps in the bearing's outer and inner parts δ_1=δ_{22}=0.00011 m.
6. Jet devices' diameters $d_{jet\ 1}$=$d_{jet\ 2}$=0.0017 m.
7. Disk console part length ℓ_{disk}=0.14 m.

The results of calculating the thickness of the disk without taking into consideration centrifugal forces are shown in Fig. 4.

These calculations demonstrate that with an increase in the diameter of the bearing, the hydrodynamic forces acting on the disk increase significantly, and, therefore, its thickness increases significantly. When the diameter of the bearing on its outer part increases from 0.091 m to 0.45 m (that is, by 5 times), the thickness of the disc increases by about 22 times.

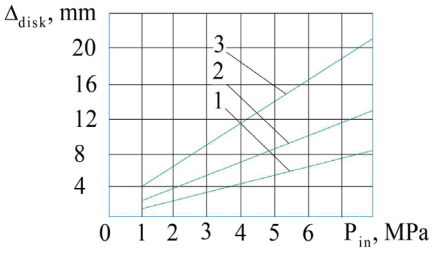

Fig. 4. The effect of feed pressure P_{in} on disk thickness Δ_{disk} for various disk's materials disregarding the centrifugal forces: 1 – steel; 2 – bronze; 3 – aluminum

5. 2. Studying the magnitude of change in the thickness of the double-type bearing disk induced by the effect of centrifugal forces in the examined range of angular velocities of the disk with a shaft

The calculation results for a large bearing, taking into consideration centrifugal forces, are shown in Fig. 5, 6.

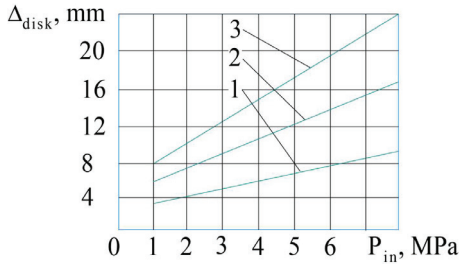

Fig. 5. The effect of feed pressure P_{in} on disk thickness Δ_{disk}, taking into consideration the centrifugal forces, at ω=314 s^{-1}: 1 – steel; 2 – bronze; 3 – aluminum

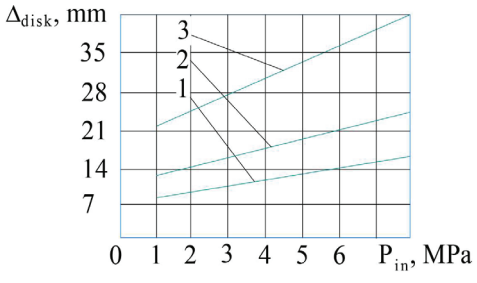

Fig. 6. The effect of feed pressure P_{in} on disk thickness Δ_{disk}, taking into consideration the centrifugal forces, at ω=628 s^{-1}: 1 – steel; 2 – bronze; 3 – aluminum

Fig. 5, 6 demonstrate that the centrifugal forces have an effect on the thickness of the bearing disk, and, with the increase in the speed of rotation of the disk with the shaft, this effect becomes significant. With an increase in the angular velocity from ω=314 s^{-1} to ω=628 s^{-1}, the required thickness of the bearing disk increases by about 1.75 times.

6. Discussion of results of studying a disk thickness

The results of the calculation of the thickness of the disk, shown in Fig. 3–6 in the form of charts, are linear in nature. Such a nature is explained by the fact that under the generally accepted assumptions in hydrodynamic lubricant theory, the dependence of hydrodynamic forces on feed pressure would be linear. This fact is confirmed by the experimental data. The resulting linear dependence of disk thickness on feed pressure explains the fact that the ratio of disk thicknesses for different materials is not dependent on feed pressure, therefore, it remains constant. A significant increase in the thickness of the disk at an increase in the frequency of its rotation (Fig. 5, 6) is due to the increasing influence of the centrifugal forces compared to hydrodynamic forces.

The proposed solutions and the results obtained could solve the task of determining the thickness of the disk through calculation, which was not available in previous studies. Determining the thickness of the disk would also significantly increase the carrying capacity of the bearing and expand the range of its stable operation.

The advantage of this study is a comprehensive approach related to solving a complex hydrodynamic problem and taking into consideration centrifugal forces.

The limitations inherent in this study are primarily related to non-temperature deformations. Not taking into consideration temperature deformations in this study was based on the fact that the operation of hydrostatic bearings is associated with high consumption. The experimental studies have shown that the temperature of a working liquid almost does not change during bearing operation. However, for powerful turbines whose bearings' diameters may equal 100 cm or larger, it may be necessary to account for temperature deformations.

The limitation of this study is that there are no experimental confirmations of the results obtained. Therefore, in the future, it is necessary to conduct experimental studies into elastic disk deformities and confirm the theoretical study reported here.

7. Conclusions

1. The suggested expression to determine the thickness of the disk, taking into consideration hydrodynamic and centrifugal forces, allowed the calculation procedure to determine the disk thickness and use it in the design of turbine supports. The results of calculating the thickness of the bearing disk without taking into consideration the centrifugal forces showed that with an increase in feed pressure from 1 MPa to 8 MPa, the thickness of the disc increases by about 4.5 times. As the feed pressure increases, the ratio of aluminum and steel thicknesses decreases. At a 1 MPa feed pressure, the steel disk is 2.5 times thicker than the aluminum disk. At a feed pressure of 8 MPa, the steel disk is 1.3 times smaller than the aluminum disk. When the diameter of the bearing on the outer part increased from 0.091 m to 0.45 m (that is, by 5 times), the thickness of the disc increased by about 26 times.

2. The results of calculating the thickness of the bearing disk, taking into consideration the centrifugal forces, showed that, despite the small thickness of the disk, the centrifugal forces must be accounted for in calculating the disk thickness. As the angular velocity increases from ω=314 rad/s to ω=628 rad/s, the required thickness of the bearing disc increased by about 2.33 times.

Reference

1. Nazin, V. (2015). Pat. No. 112922 UA. Radialnyi hidrostatodynamichnyi kombinovanyi pidshypnyk. No. a201503374; declareted: 10.04.2015; published: 10.11.2016, Bul. No. 21.
2. Nazin, V. (2012). Radial hydrostatical bearing of enhanceable bearing strength. Aerospace technic and technology, 8 (95), 94–100.
3. Nazin, V. (2015). Sravnenie dinamicheskih harakteristik sdvoennyh i odinarnyh gidrostatodinamicheskih podshipnikov. Aerospace technic and technology, 9 (126), 85–88.
4. Avishai, D., Morel, G. (2021). Experimental Investigation of Lubrication Regimes of a Water-Lubricated Bearing in the Propulsion Train of a Marine Vessel. Journal of Tribology, 143 (4). doi: https://doi.org/10.1115/1.4048382
5. Koosha, R., San Andr s, L. (2020). A Computational Model for the Analysis of the Static Forced Performance of Self-Equalizing Tilting Pad Thrust Bearings. Journal of Engineering for Gas Turbines and Power, 142 (10). doi: https://doi.org/10.1115/1.4048458

6. Amann, T., Chen, W., Baur, M., Kailer, A., Rühe, J. (2020). Entwicklung von galvanisch gekoppelten Gleitlagern zur Reduzierung von Reibung und Verschleiß. Forschung Im Ingenieurwesen, 84 (4), 315–322. doi: https://doi.org/10.1007/s10010-020-00416-z
7. Gheisari, R., Lan, P., Polycarpou, A. A. (2020). Efficacy of surface microtexturing in enhancing the tribological performance of polymeric surfaces under starved lubricated conditions. Wear, 444-445, 203162. doi: https://doi.org/10.1016/j.wear.2019.203162
8. Liu, Y., Zou, J., Deng, Y., Ji, H. (2020). Research on the seawater-lubricated sliding bearing of a novel buoyancy-regulating seawater pump considering the working depth. Australian Journal of Mechanical Engineering, 1–20. doi: https://doi.org/10.1080/14484846.2020.1716510
9. Zhao, Y., Jianxi, Y. (2019). Influence of interface slip on the surface frictional force of texturing sliding bearing. Industrial Lubrication and Tribology, 72 (6), 735–742. doi: https://doi.org/10.1108/ilt-01-2018-0032
10. Polyakov, R., Savin, L., Fetisov, A. (2018). Analysis of the conditions for the occurrence of the effect of a minimum of friction in hybrid bearings based on the load separation principle. Proceedings of the Institution of Mechanical Engineers, Part J: Journal of Engineering Tribology, 233 (2), 271–280. doi: https://doi.org/10.1177/1350650118777143
11. Syed, I., Sarangi, M. (2018). Combined effects of fluid–solid interfacial slip and fluid inertia on the hydrodynamic performance of square shape textured parallel sliding contacts. Journal of the Brazilian Society of Mechanical Sciences and Engineering, 40 (6). doi: https://doi.org/10.1007/s40430-018-1241-2
12. Zernin, M. V., Mishin, A. V., Rybkin, N. N., Shil'ko, S. V., Ryabchenko, T. V. (2017). Consideration of the multizone hydrodynamic friction, the misalignment of axes, and the contact compliance of a shaft and a bush of sliding bearings. Journal of Friction and Wear, 38 (3), 242–251. doi: https://doi.org/10.3103/s1068366617030163
13. Zhang, J., Tan, A., Spikes, H. (2016). Effect of Base Oil Structure on Elastohydrodynamic Friction. Tribology Letters, 65 (1). doi: https://doi.org/10.1007/s11249-016-0791-7
14. Nazin, V. (2020). Influence mass of the rings, resiliently set on disk, on dynamic descriptions of hydrostatodynamic bearing of the doubled type. Aerospace technic and technology, 8 (168), 100–105. doi: https://doi.org/10.32620/aktt.2020.8.13
15. Nazin, V. I. (2013). Theory of double radial bearing in gidrostatodinamicheskogo stationary external load. Aerospace technic and technology. Aerospace technic and technology, 8 (105), 160–166.
16. Constantinescu, V. N. (1959). On Turbulent Lubrication. Proceedings of the Institution of Mechanical Engineers, 173 (1), 881–900. doi: https://doi.org/10.1243/pime_proc_1959_173_068_02
17. Konstantinesku, V. N. (1974). Gidrodinamicheskaya smazka: turbulentnost' i rodstvennye yavleniya. Materialy obschey diskussii na simpoziume ASME. Tr. amerik. obsch. inzh.-mekh. Problemy treniya i smazki. Ser. F, 96 (1), 198–208.
18. Tipey, N., Konstantinesku, V. N., Nika, A., Bitse, O. (1964). Podshipniki skol'zheniya (raschet, proektirovanie, smazka). Buharest: Izdatel'stvo Akad. Rum. Nar. Resp., 457.
19. Krylov, V. I., Babkov, V. V., Monastyrniy, P. I. (1977). Vychislitel'nye metody. Vol. 2. Moscow: Nauka, 400.